Small Animal PET Imaging

Gary D. Hutchins, Michael A. Miller, Victor C. Soon, Timothy Receveur

Abstract

Positron emission tomography (PET) is well established as an important research and clinical molecular imaging modality. Although the size differences between humans and rodents create formidable challenges for the application of PET imaging in small animals, advances in technology over the past several years have enabled the translation of this imaging modality to preclinical applications. In this article we discuss the basic principles of PET instrumentation and radiopharmaceuticals, and examine the key factors responsible for the qualitative and quantitative imaging capabilities of small animal PET systems. We describe the criteria that PET imaging agents must meet, and provide examples of small animal PET imaging to give the reader a broad perspective on the capabilities and limitations of this evolving technology. A crucial driver for future advances in PET imaging is the availability of molecular imaging probes labeled with positron-emitting radionuclides. The strong translational science potential of small animal and human PET holds great promise to dramatically advance our understanding of human disease. The assessment of molecular and functional processes using imaging agents as either direct or surrogate biomarkers will ultimately enable the characterization of disease expression in individual patients and thus facilitate tailored treatment plans that can be monitored for their effectiveness in each subject.

Key Words: positron emission tomography; radiopharmaceuticals; sensitivity; small animal; small animal PET; spatial resolution

Introduction

Positron emission tomography (PET[1]) is a noninvasive molecular imaging modality that measures the in vivo biodistribution of imaging agents labeled with positron-emitting radionuclides. The principal goal of PET imaging is to characterize biological processes in tissues and organs with minimally invasive procedures (Phelps 2000a). This technology, originally developed and tested in the 1960s, has evolved into an invaluable research tool and in recent years has developed into an important clinical imaging modality as well (Cherry et al. 2003; Hoffman and Phelps 1976; Muehllehner and Karp 2006; Phelps 2000b; Wahl and Buchanan 2002).

The development of targeted positron-emitting molecular imaging agents enables both the qualitative and quantitative assessment of numerous biological processes including perfusion, metabolism, protein expression, and enzyme activity. This diverse array of available molecular imaging agents, coupled with advanced data analysis methods, supports the application of PET for the assessment of normal biological processes, the assessment of changes in biological processes associated with disease formation and progression, and the ability to monitor the response of healthy and diseased tissue to therapeutic intervention. PET imaging is also utilized in the drug discovery process to provide information about novel drug biodistribution, drug occupancy at specific biological targets, and biological response to drug exposure (Cherry 2001a,b; Paans and Vaalburg 2000; Vaalburg 1999).

PET imaging technology has advanced rapidly over the past decade and now provides a previously unimagined capacity to visualize, quantify, and study the living function of human and mammalian tissues and organs. Technological advances in PET instrumentation have enabled the translation of human and large animal PET imaging capabilities to the scale of small animals (Bloomfield et al. 1997; Cherry 2006; Cherry et al. 1997; Cutler et al. 1992; Del Guerra et al. 1998; Jeavons et al. 1999; Lecomte et al. 1996; Marriott et al. 1994; Rouze and Hutchins 2003, Rouze et al. 2003; Seidel et al. 2003; Surti et al. 2005; Tai et al. 2001, 2003, 2005; Watanabe et al. 1992, 1997; Weber et al. 1997; Ziegler et al. 2001). The current generation of small animal PET imaging systems can achieve spatial resolution in the 1- to 2-mm full-width-at-half-maximum (FWHM[1]) range with point source detection sensitivities in the 1% to 15% range, providing image quality in small animals that is beginning to approach the qualitative and quantitative capabilities of human PET imaging (Tai and Laforest 2005; Weber and Bauer 2004).

Gary D. Hutchins, PhD, is John W. Beeler Professor; Michael A. Miller, PhD, is an assistant research professor; Victor C. Soon, PhD, is a hardware and software engineer; and Timothy Receveur, MS, is a data analyst, all in the Department of Radiology at the Indiana University School of Medicine in Indianapolis.

Address correspondence and reprint requests to Dr. Gary D. Hutchins, Department of Radiology, Indiana University School of Medicine, 950 West Walnut Street—R2, I124, Indianapolis, IN 46202-5181 or email gdhutchi@iupui.edu.

[1]Abbreviations used in this article: FDG, 2-[F-18]fluoro-2-deoxy-D-glucose; FWHM, full-width-at-half-maximum; keV, kiloelectron volt; PET, positron emission tomography; RMSE, root mean square error

The ability to adopt molecular and functional imaging technologies for applications in both the preclinical and clinical settings provides a bidirectional conduit for the translation of knowledge and novel technologies between these research settings. Many human PET imaging methods have proved to be quantitative, highly sensitive (detection down to picomolar and nanomolar concentration ranges), useful in measuring tracer kinetics, repeatable and reproducible, and minimally invasive, making them well suited for clinical research applications (Wolbarst and Hendee 2006). Methods validated in the human and large animal imaging setting are being translated to the small animal setting. As a result, it is now possible to translate biological knowledge gained in the small animal setting with these technologies for application in clinical procedures with analogous methods for the study of human biology and biochemistry.

This bidirectional translational science tool (Figure 1) holds great promise to dramatically advance our understanding of human disease. The assessment of molecular and functional processes using imaging agents as either direct or surrogate biomarkers will ultimately enable the characterization of disease expression in individual patients and thus facilitate tailored treatment plans that can be monitored for their effectiveness in each subject (McLarty and Reilly 2007).

In this short review of PET imaging technologies for small animal imaging we provide an overview of the principles of PET imaging, describe challenges and limitations inherent in the application of PET imaging to small animals, discuss the characteristics to consider in the selection of radiopharmaceuticals, and offer examples of imaging applications from our laboratory. Our objective is to provide the reader with an understanding of PET imaging and its application in small animal models.

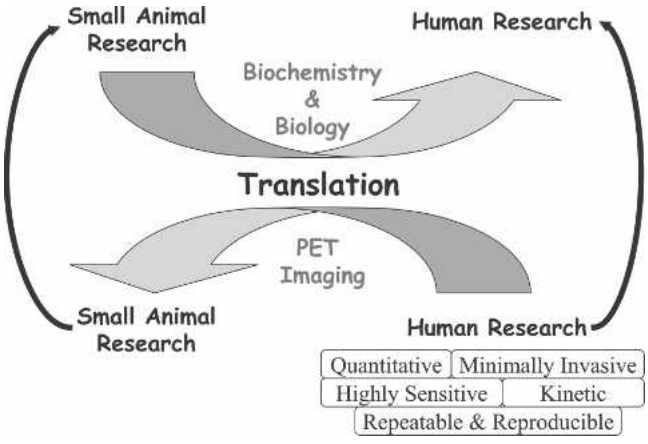

Figure 1 Bidirectional translational science with human and small animal PET imaging. Methods for human PET have been well characterized and shown to have high detection sensitivity and to be quantitative, minimally invasive, capable of measuring imaging agent kinetics, and highly repeatable and reproducible. Recent advances in PET imaging technology have enabled the translation of this technology for application in small animals. The combination of human and small animal PET imaging technologies now permits a bidirectional translational science approach, where advances in technology and methodology help enhance understanding of human biochemistry and biology.

Principles of PET Imaging

Positron Decay

PET imaging systems detect the 511-kiloelectron volt (keV[1]) annihilation photons generated as a result of positron decay by unstable proton-rich radionuclides (Phelps et al. 1975). Such nuclei achieve stability either by electron capture (in which the nucleus captures a nearby orbital electron) or by emission of a positron (a particle with the same mass and spin as an electron but with a positive charge). Positrons emitted in this decay process are released with kinetic energy that follows a distribution that is characteristic of each radionuclide. Once emitted from the nucleus the positron loses its kinetic energy through electrostatic interactions with neighboring charged particles (electrons and protons) as it moves through the surrounding environment. As its kinetic energy transfers to the surrounding material, the positron slows and eventually combines with a nearby electron to form an ultrashort-lived entity called positronium (Harpen 2004). The rapid annihilation of positronium produces two 511-keV annihilation photons that are emitted in opposite directions due to conservation of energy and momentum. The annihilation process is depicted graphically in Figure 2. The annihilation photons are gamma rays that can be detected by numerous types of radiation detectors. The distance traveled by the positron before the formation and subsequent annihilation of positronium is the positron range. Table 1 lists the average positron energy and positron range in soft tissue for both common and less commonly used positron-emitting radionuclides.

Detection of Annihilation Photons

Positron emission results in annihilation photons that are nearly 180° opposed and travel at the speed of light (30 cm/ns). PET scanners use pairs of radiation detectors to measure the nearly simultaneous, coincident interaction of the 511-keV photons. Detector pairs are normally arranged in geometric shapes that approximate a circle in 2D and a cylinder in 3D (Figure 2). The line that connects any two detectors in the PET scanner is called a line of response. In a typical PET study the scanner measures on the order of 0 to 100 events in any one line of response.

Once the events are collected, mathematical tomographic image reconstruction algorithms transform them into an image that represents a slice through the object in the

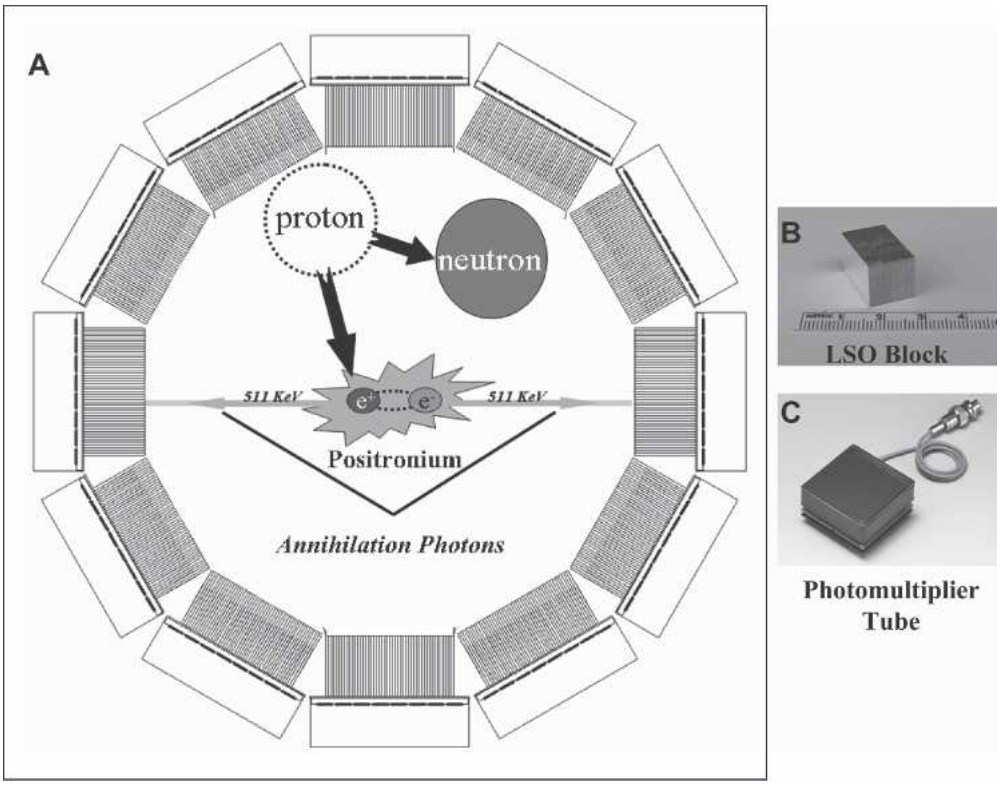

Figure 2 PET scanner detector geometry and positron emission. (A) A PET scanner measures the signal that results from positron (e^+) emission, which occurs when an unstable nucleus decays by emitting a positron, converting a proton to a neutron. The emitted positron combines with an electron to form the ultrashort-lived positronium. Positronium annihilation (mass is converted into energy) creates two 511-keV annihilation photons that are emitted approximately 180° opposed to one another. PET scanners consist of radiation detectors arranged in a geometry that approximates a cylindrical shape. The most common detector type is a block detector, which consists of 50 or more individual elements, or crystals, made of scintillation material, and electronics that determine which individual crystal was struck by a photon. The individual detector elements in the PET scanner operate in coincidence to detect the 511-keV annihilation photons. The detection of coincidence events identifies a line of response in which the decay occurred. This figure also shows a sample lutetium oxyorthosilicate (LSO) inorganic scintillator block of crystals (B) and (C) a photomultiplier tube coupled to the detector block to collect scintillation light for crystal identification.

plane of the detector ring. Many image reconstruction algorithms are currently in use with PET scanners, including (but not limited to) filtered backprojection, expectation maximization (EM), ordered subset expectation maximization (OSEM), and maximum a posteriori (MAP). There are many tradeoffs to consider when selecting these algorithms for use in imaging studies. A careful consideration of the relative advantages of PET reconstruction algorithms is beyond the scope of this article; we refer the interested reader to review articles by Defrise and Gullberg (2006), Lewitt and Matej (2003), and Qi and Leahy (2006).

PET Detectors

The key factors that determine the performance of a PET scanner include (Tai and Laforest 2005):

Table 1 Positron emitter average energy and positron range in soft tissue[a]

Radionuclide	^{11}C	^{13}N	^{15}O	^{18}F	^{62}Cu	^{64}Cu	^{82}Rb	^{94m}Tc	^{124}I
$Energy_{avg}$ (MeV)	0.386	0.492	0.735	0.250	1.315	0.278	1.475	1.072	0.818
$Range_{avg}$ (mm)	1.52	2.05	3.28	0.83	6.21	0.97	7.02	4.98	3.70

[a]Data from Tai YC, Laforest R. 2005. Instrumentation aspects of animal PET. Ann Rev Biomed Eng 7:255-285.

- detection efficiency: probability that a 511-keV photon will interact with the detector;
- spatial resolution: ability to localize detected 511-keV photons;
- resolving time: ability of the detector to accurately determine the time of 511-keV photon arrival;
- energy resolution: ability to differentiate between primary 511-keV photons and lower-energy photons scattered before detection; and
- count rate capabilities: ability of the detector to process events in rapid succession.

Major research efforts over the past 20 years have sought to identify the optimal detector materials for both human and small animal PET scanners. The most prominent choice of detector material for PET imaging has been inorganic scintillators. As implied by their name these crystalline materials scintillate after a 511-keV photon interaction (Knoll 1979), causing the formation of photoelectric and/or Compton electrons, which in turn result in electrons in the crystal lattice being left in excited states. The electrons in the excited states move to lower energy levels in the crystalline structure and thus release energy in the form of fluorescence, which can be detected by secondary photon detectors (such as photomultiplier tubes and avalanche photodiodes). The physical properties of many of the inorganic scintillators that have been incorporated in PET scanner designs are provided in Table 2. Figure 2 shows a photograph of the lutetium oxyorthosilicate (LSO) inorganic block scintillator and Hamamatsu photomultiplier tubes used in a small animal PET scanner developed in our laboratory (Rouze et al. 2003).

PET Image Spatial Resolution

Several factors govern the achievable spatial resolution in a PET imaging system. Derenzo and Moses (1993) have developed a parameterized expression that relates the relative contribution of each of these factors to the observed spatial resolution. Spatial resolution in PET imaging systems is typically characterized as the full-width-at-half-maximum (FWHM) of a profile that runs through the center of a point or perpendicular to a line source image. The parameterized expression of PET spatial resolution is

$$\mathrm{FWHM} = \alpha\left[\left(\frac{d}{2}\right)^2 + b^2 + (0.0022D)^2 + r^2\right]^{\frac{1}{2}} \qquad (1)$$

The first term inside the square brackets is related to the geometry of the individual detector crystals, where d is the dimension of the square face of a crystal. In most PET scanners the size of the crystal is a dominant component of the achievable spatial resolution. The second term inside the brackets, parameterized by b, represents the uncertainty associated with identifying individual crystals with secondary detection devices such as photomultiplier tubes. This factor typically contributes only a fraction of a millimeter to the spatial resolution. The third term inside the brackets $[(0.0022D)^2]$ describes the noncolinearity of the 511-keV photons (due to the small kinetic energy of the positronium, the two photons are not emitted exactly back to back along colinear paths but along noncolinear paths slightly less than 180° apart). The spatial resolution degradation caused by noncolinearity is dependent on the spacing between the detectors (D), which are operated in coincidence. For the imaging geometries used in small animal PET scanners this factor typically is less than 0.5 mm FWHM. The last term in this expression relates to the effective size of the object, which includes the positron range factors discussed above (see Table 1). Finally, the multiplicative factor α accounts for resolution degradation that occurs in the image reconstruction process; for conventional filtered backprojection reconstruction algorithms this term is typically set to 1.2.

Table 2 Physical and optical properties of PET scintillation materials[a]

Scintillation material[b]	Density (g/cm^3)	Effective atomic number (Z)	Primary decay constant (ns)	Emission intensity (% relative to NaI)	Emission wavelength (nm)	Attenuation coefficient at 511 keV (cm^{-1})
NaI(Tl)	3.67	51	230	100	410	0.35
LSO	7.40	65	40	75	420	0.86
GSO	6.71	59	60	30	430	0.70
BGO	7.13	75	300	15	480	0.95
YAP	5.55	32	27	40	350	0.37
BaF_2	4.88	53	2	12	220, 310	0.45
YSO	4.45	36	70	45	550	0.36
LuAP	8.34	64	17	30	365	0.87

[a]Data from Tai YC, Laforest R. 2005. Instrumentation aspects of animal PET. Ann Rev Biomed Eng 7:255-285.
[b]LSO (Lu_2SiO_5:Ce), GSO (Gd_2SiO_5:Ce), BGO ($Bi_4Ge_3O_{12}$), YAP ($YAlO_3$:Ce), YSO (Y_2SiO_5), LuAP ($LuAlO_3$:Ce).

Spatial resolution affects the level of detail that can be visualized in an image and limits the size of structures for which accurate quantification of radionuclide concentrations can be achieved (Hoffman et al. 1979). If an object is smaller (in any dimension) than approximately 2.5 × FWHM spatial resolution of the PET scanner, a distortion called partial volume effect occurs. This term describes the condition in which the cross-sectional area of the object being imaged is smaller than that of the sensitive region of the detector pairs used to detect the 511-keV annihilation photons. Partial volume distortions lead to biased quantitative estimates of tracer concentration in the tissue in an object size–dependent fashion.

Figure 3 plots recovery coefficient (ratio of observed tracer concentration to true) values versus volume of a spherical object for multiple FWHM spatial resolution values encompassing the range of values observed in modern-generation small animal PET systems. The plot includes an indication of the size of major organs in rats and mice. Figure 3 shows the feasibility of reliable assessments of PET tracer concentrations in the whole organs of rats and mice. The ability to produce unbiased quantitative PET images of tracer concentration in substructures of the major organs or in situations in which the tracer concentration is heterogeneous in the regional volume (e.g., in a tumor) is strongly dependent on the spatial resolution of the PET scanner and the geometrical distribution of the PET imaging agent.

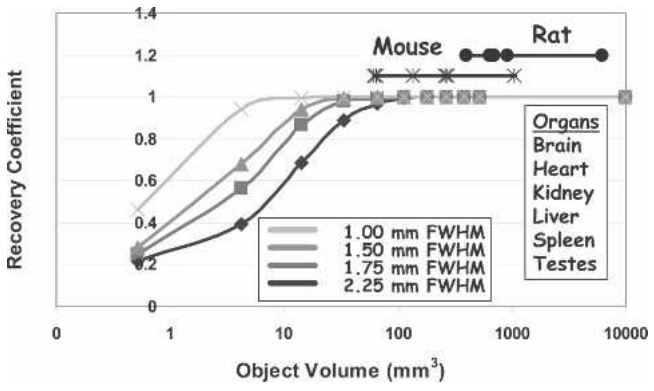

Figure 3 PET image recovery coefficient vs. spherical object volume. The partial volume effect distorts the signal intensity of small objects; in this figure the recovery coefficient represents the resulting fractional distortion. Recovery coefficient values are plotted for spherical objects as a function of imaging system full-width-at-half maximum (FWHM) spatial resolution. Overlaid on the plot are organ volumes in the mouse (stars) and rat (circles), demonstrating that minimal partial volume effects are expected for whole organ volumes assuming the radionuclide uptake is uniform in the organ. Each overlaid point represents one of the organs in the legend, ordered from largest to smallest volume. The four curves in the plot represent imaging systems with FWHM spatial resolution values of 1.0, 1.5, 1.75, and 2.25 mm.

Sensitivity

The decay of positron-emitting radionuclides is a random process. Consequently the lines of response measured by the PET scanner represent one sample from a Poisson distribution with a mean value that represents the total quantity of radionuclide between the pair of detectors. In order to minimize the uncertainty in each line of response measurement it is necessary to maximize the total number of coincidence events detected. The system sensitivity is the efficiency with which the PET scanner detects a coincidence event when a radionuclide located in the field of view of the scanner emits a positron. The sensitivity of PET scanners is often quoted as the percentage of events detected from a small spherical source placed at the geometric center of the sensitive volume of the PET scanner.

Quantification of Biological Processes

Human and small animal PET technologies, when properly calibrated, provide quantitative images of radionuclide concentrations. There are a number of methods to convert these quantitative image datasets into estimates of tissue biology (such as perfusion and metabolic rate) or estimates of protein concentrations and ligand binding characteristics. Most of these techniques require the acquisition of a temporal sequence of images in order to characterize regional PET tracer kinetics. Knowledge of the time course of the PET tracer concentration in the arterial blood is often also necessary as an input function to mathematical tracer kinetic models that are fit to regional tissue time activity curves providing estimates of biological parameters. Although beyond the scope of this article, the logistics of performing these studies are more complex than in human studies due to the size of the animal being studied.

Challenges and Limitations of Small Animal PET

Spatial Resolution

Relative volumetric differences in organs and tissues between humans and small animals create formidable challenges for PET imaging. The human/mouse and human/rat mass scale factors typically fall in the range of 2,500 to 3,750 and 250 to 375 respectively. In addition, organ/whole body mass ratios can vary dramatically across species by up to a factor of 4. In comparison, the volumetric resolution improvement factor for dedicated small animal PET scanners relative to current state-of-the-art human PET scanners falls in the range of 30 to 125. Consequently, under the best-case scenario (i.e., larger small animals), the ratio of the volumetric spatial resolution to animal mass is approximately a factor of 30 times lower for mice and 3 times lower for rats than in human PET imaging.

To put the small animal imaging capabilities in perspective with human imaging, a plot of the equivalent spatial resolution achievable in a human imaging study is contrasted with small animal PET spatial resolution in Figure 4. This figure also provides simulation images to help assess image quality relative to human imaging. The predominant factors that determine small animal PET spatial resolution are the detector element size (*d* in equation 1) and the positron range (*r* in equation 1; also see Table 2).

Sensitivity

The importance of maximizing system sensitivity and total number of detected events can be demonstrated using an empirically derived expression for the root mean square error (RMSE[1]) in a resolution cell of a tomographically reconstructed image. The RMSE, the square root of the mean squared difference between the known value and the measured value, is a measure of the accuracy of an image: the smaller the RMSE, the more accurately the image represents the object. Budinger and colleagues (1978) calculated the RMSE of a resolution cell of a tomographically reconstructed image as

$$\mathrm{RMSE} = 1.2\left[M_t + \frac{M_b}{C}\right]^{\frac{3}{4}} N^{-\frac{1}{2}} \qquad (2)$$

In this equation, M_t and M_b are the number of resolution cells in the target and background respectively, C is the ratio of target-to-background tracer concentration (the contrast ratio), and N is the total number of recorded 511-keV photon pairs from positron decays. A resolution cell is a cubic volume that represents the PET system spatial resolution in each dimension.

Figure 5 illustrates the relationship between RMSE in a resolution cell and PET scanner FWHM resolution for a mouse torso geometry with a 5-mm tumor that has a 5:1 tumor-to-background contrast ratio. Reduction of the RMSE at high spatial resolution is possible only through an increase in the number of detected coincidence events or through the development of reconstruction algorithms that are less sensitive to the noise in the measured data. Miller and colleagues (2003) have shown that if one accounts for the relative organ size differences across species (assuming that PET tracer distribution across organs is similar between humans and rodents), then it is possible to calculate a set of scale factors to determine the radiotracer dose level needed in a rat or mouse to achieve image signal-to-noise characteristics similar to those observed in human PET studies. Figure 6 plots the human/rodent dose scale factors versus the concentration scale factor (labeled and nonlabeled imaging agent) that occurs as a function of image spatial resolution.

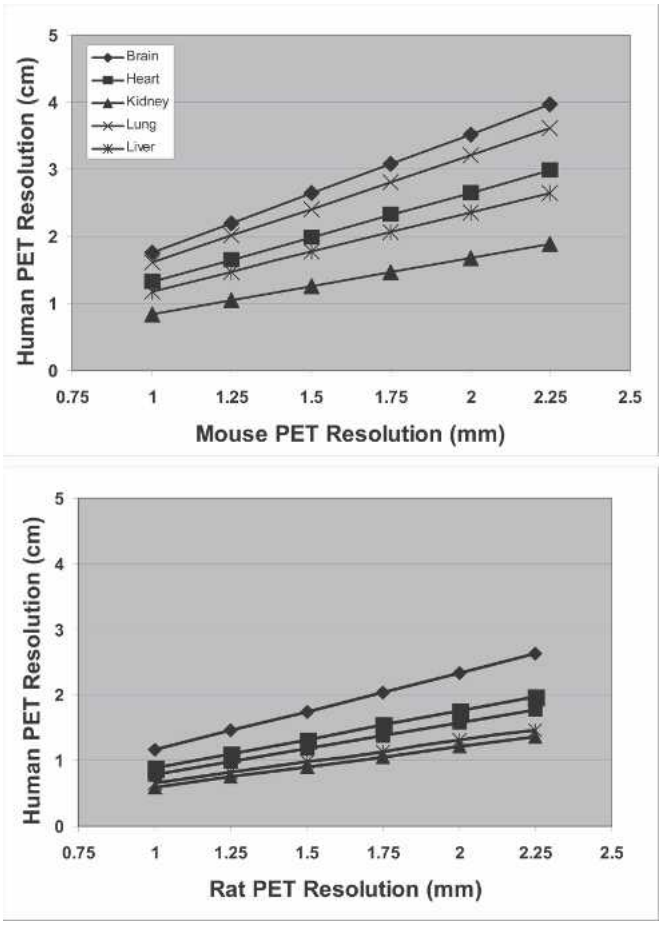

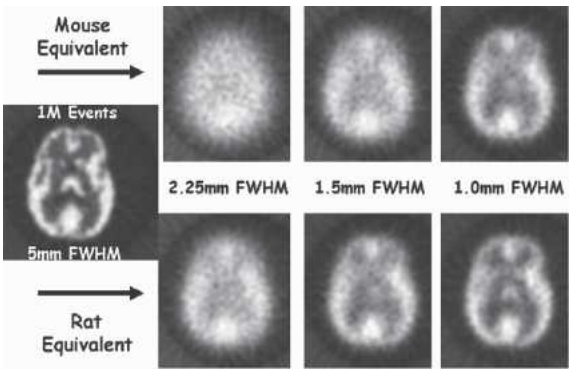

Figure 4 Relative spatial resolution in humans. The plots in this figure provide an estimate of the effective human PET image resolution that would be achieved if the total number of resolution elements in the rat (lower plot) and mouse (upper plot) organs were achieved in human studies. The image immediately to the right of the upper plot is a brain image transaxial slice at 5 mm full-width-at-half maximum (FWHM) in a human PET scanner. The remainder of the images on the right side of the figure show what the human brain image would look like if it were scaled to the rat or mouse brain size and imaged at 1, 1.5, or 2.25 mm FWHM resolution. These images show that, as the small animal PET FWHM spatial resolution reaches 1.5 mm or better, the image quality begins to approach the image quality observed in human PET imaging studies.

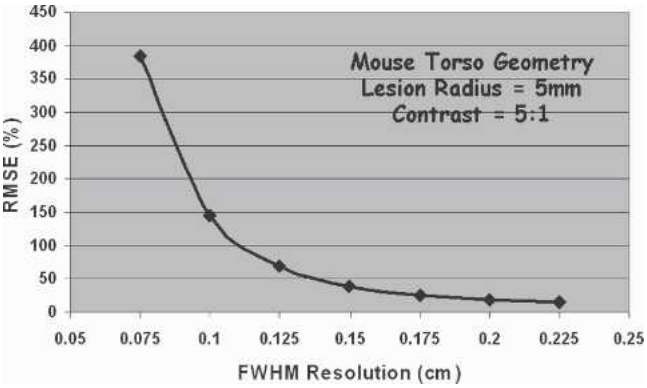

Figure 5 Root mean square error (RMSE) in a resolution cell. The plot represents the RMSE of a simulated tumor in a mouse torso. The tumor was 5 mm in diameter and had a 5:1 contrast relative to the surrounding background. Note the rapid increase in RMSE, and decrease in FWHM resolution, as the spatial resolution improves. To take advantage of this, the image data must be reconstructed into smaller image elements (or voxels); smaller voxels result in less PET tracer per voxel and therefore less signal and more noise.

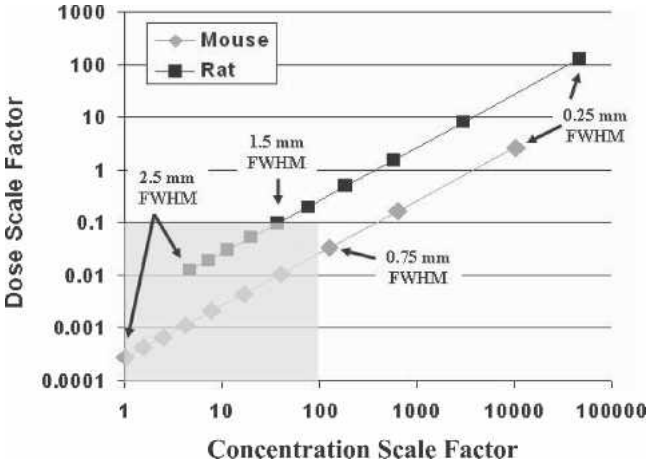

Figure 6 Dose vs. concentration scale factors associated with achieving small animal PET imaging quality equivalent to human PET image quality. The ordinate of this plot represents the approximate fraction of a human PET dose necessary to achieve equivalent image root mean square error (RMSE) as a 5 mm full-width-at-half maximum (FWHM) human PET image. The abscissa of this plot is the scale factor for the in vivo imaging agent concentration (labeled and nonlabeled) that occurs when going from a human administration to a rodent administration. The individual data points on each curve represent a specific small animal PET FWHM spatial resolution (from 0.25 mm to 2.5 mm FWHM in 0.25-mm increments). The shaded region on the plot represents approximate limits for achievable spatial resolution when taking multiple imaging factors into consideration (i.e., radionuclide concentration limits for PET scanners, nonlabeled imaging agent concentration limits, and practical image acquisition durations). The radiopharmaceutical dose used in human studies is agent specific and typically falls in the range of 185 to 1850 MBq; typical rodent radiopharmaceutical doses are in the range of 3.7 to 37 MBq. In these dose ranges the total imaging agent concentration (labeled and nonlabeled) can approach 100 times the concentration observed in human tissues during PET studies. This plot can be used to estimate the tracer dose required to image small animals with image quality similar to that achieved in clinical human imaging. For example, to image a rat in a system with 1.5 mm FWHM resolution and achieve RMSE characteristics similar to those observed in human images, the total dose required would be 0.1 times the clinical dose and would result in about 50 times the imaging agent concentration.

Radiation Exposure

The radiation exposure that results from a clinical 2-[^{18}F]fluoro-2-deoxy-D-glucose (FDG[1]) PET scan of a human is approximately 7 millisieverts (mSv), about half that required for a whole body diagnostic x-ray CT image (Brix et al. 2005). For a radioactivity concentration similar to that used in human clinical studies, the radiation dose to a rat is approximately 20% of the human radiation dose, or 1.4 mSv. This radiation dose scale factor is approximately 10% for a mouse, resulting in a radiation dose of 0.7 mSv. If the tracer concentration scale factor shown in Figure 6 is taken into account, these radiation doses increase by a factor of 1 to 100, leading to radiation doses of 0.7 to 140 mSv, depending on the image quality and resolution. The dose for a small animal imaging study is ultimately limited by the count rate capabilities of the PET detectors, the radiation exposure to the animal, and the specific activity of the PET tracer.

PET Radiopharmaceuticals

The feasibility of small animal PET imaging is critically dependent on instrumentation that can produce images with both the spatial resolution and detection sensitivity consistent with the size of the animal and the organ or tissues being studied. However, the success of human and small animal PET is also contingent on positron-emitting imaging agents that have the appropriate pharmacokinetic properties to enable characterization of specific biological processes.

There are multiple types of mechanisms that lead to the uptake and retention of PET imaging agents. In general terms, these mechanisms can be characterized as either saturable or nonsaturable. A PET imaging agent that provides desired information about a biological process must meet the following general criteria, contingent on whether the uptake and retention mechanisms are saturable or nonsaturable (Elsinga et al. 1998; van Waarde et al. 1995):

- Tracer: The PET imaging agent should be present in a very low concentration so that it does not perturb the biological process under study.
- Saturability: The protein target site of the PET imaging agent can be saturated with a large mass of unlabeled agent or with an agonist or antagonist that interacts with the target. If saturability cannot be demonstrated, the

accumulation of tracer is unlikely to reflect interaction with the protein target.

- Specificity: Ideally the PET imaging agent will interact only with a specific protein site. If interaction with multiple sites occurs, isolation of the specific site of interest from competing interactions becomes extremely difficult.
- Stereoselectivity: Interaction of the PET imaging agent with the target site depends on the conformational orientation of the molecule. Nonspecific binding of the tracer tends to occur independent of the conformational orientation of the molecule.
- Affinity: High affinity for the target site is typically necessary in order to generate good contrast between the target and nonspecific sites of PET imaging agent accumulation.
- Biodistribution: The regional distribution of the imaging agent must permit the delineation of the target organ or tissue from the surrounding tissues.
- Correlation with biologic effect: The accumulation, retention, and/or binding of the PET imaging agent should correlate with biological responses specific to the system under study.
- Resistance to metabolism: PET imaging systems measure the distribution of the positron-emitting radionuclide. If the administered imaging agent is metabolized by the body the PET signal is derived from multiple molecules, confounding the ability to assess the biology of the specific process of interest. Thus tracers that are not metabolized, or those with metabolic products that are sequestered in the cell where the original physiological process under study occurred, are desirable.
- Pharmacokinetics: Successful PET imaging agents have in vivo kinetic properties that are rate limited by key steps in the biological process of interest. If the rate-limiting step in the in vivo kinetics of the PET imaging agent is not associated with the biological process of interest then it becomes very difficult and often impossible to obtain useful information about the process of interest.
- Toxicity: PET imaging agents (including nonradiolabeled parent compound) should not be toxic at the low levels typically administered for imaging studies (10^2 pm to 10^2 nm).

Many PET tracers meet these criteria for human imaging applications, and most of them are labeled with ^{11}C and ^{18}F. As these agents are employed in small animal imaging studies, it is essential to consider the specific activity (positron-emitting radionuclide quantity per mass of imaging agent, labeled and nonlabeled) (Hume and Myers 2002; Jagoda et al. 2004; Kung and Kung 2005; Sossi and Ruth 2005). Hume and his colleagues estimate that a specific activity on the order of 37 MBq/μmol is required when studying saturable protein sites in small animals. Figure 7 shows this consideration for imaging studies of D2 receptor sites in rats using the D2 receptor antagonist [^{11}C]raclopride

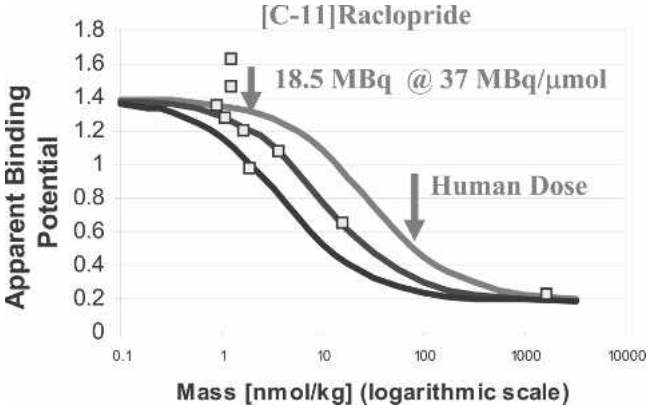

Figure 7 Specific activity considerations in [^{11}C]raclopride small animal PET studies. The solid lines represent models of the apparent binding potential versus raclopride mass that one would expect to observe in PET studies. The squares are measured binding potentials observed in control animals studied in our laboratory. The two arrows represent the expected observation with an 18.5 MBq injection (at a specific activity of 37 MBq/μmol) in rats and the binding potential that would be observed with the administration of a human dose (approx 74 MBq). These data nicely demonstrate that a specific activity of 37 MBq/μmol and a relatively small injected dose of [^{11}C]raclopride is necessary to obtain accurate estimates of available dopamine D2 receptors (binding potential).

(G.H. personal communication with Evan Morris, Assistant Professor, Indiana University—Purdue University Indianapolis, July 19, 2007).

Current efforts to develop PET tracers fall into two general areas: those in which tracers serve as surrogates for invasive or histological measurements of biological processes (such as perfusion, metabolism, or reporter probe expression) and those in which tracers target specific aspects of a biological process (such as enzyme activity, receptor concentration, uptake transporter concentration, or protein synthesis) (Sossi and Ruth 2005). The complex research required to identify candidate compounds, develop synthetic labeling methods, and demonstrate that the candidate imaging agent meets the criteria defined above is a major impediment to the rapid implementation of PET methods for the study of specific biological processes.

Applications

Small animal imaging can be applied to study any organ or tissue whose physical dimensions are consistent with the spatial resolution of the PET scanner. We provide examples from studies performed on the small animal PET system at Indiana University (IU). This system has a spatial resolution of approximately 1.1 mm FWHM in the center of the field of view and a point source detection sensitivity approaching 6%. All imaging examples were acquired with IU Animal Care and Use Committee approval. In each example the

images were reconstructed using an in-house-developed filtered backprojection reconstruction algorithm.

Figure 8 shows the whole body distribution of FDG in a 20-g mouse. FDG is a PET tracer that is retained in relationship to the rate at which glucose is transported into the cell, enters the glycolytic pathway, and is phosphorylated by hexokinase. After phosphorylation by hexokinase, FDG is trapped in most cells. Therefore, accumulation and retention of FDG are high in tissue with high glucose metabolic rates (e.g., the brain and myocardium).

The FDG tracer administration for the images in Figure 8 was performed while the animal was awake. The animal remained awake for 45 minutes after injection to permit the tracer to be delivered throughout the body and trapped via the glycolytic pathway. At 45 minutes the animal was anesthetized with isoflurane and placed in the PET scanner for imaging. The whole body images shown in Figure 8 (C, D) were acquired for 15 minutes and reconstructed with an in-house image reconstruction algorithm.

Figure 9 shows [F-18]fluoride retention in the skeleton of a 200-g Sprague-Dawley rat that received the bone-seeking agent $Na^{18}F$. Images were acquired 15 minutes after the injection of the PET tracer. The images in this figure are maximum intensity projection images in the coronal and sagittal views, providing a 3-dimensional context to the images. Maximum intensity projections (MIPs) are projections of a 3-dimensional dataset onto an image plane. Each pixel of a MIP represents the maximum intensity of the image volume along the projection direction. In PET this highlights regions and structures of high tracer retention. The ability of state-of-the-art small animal PET imaging systems to capture fine structural detail is evident in these images.

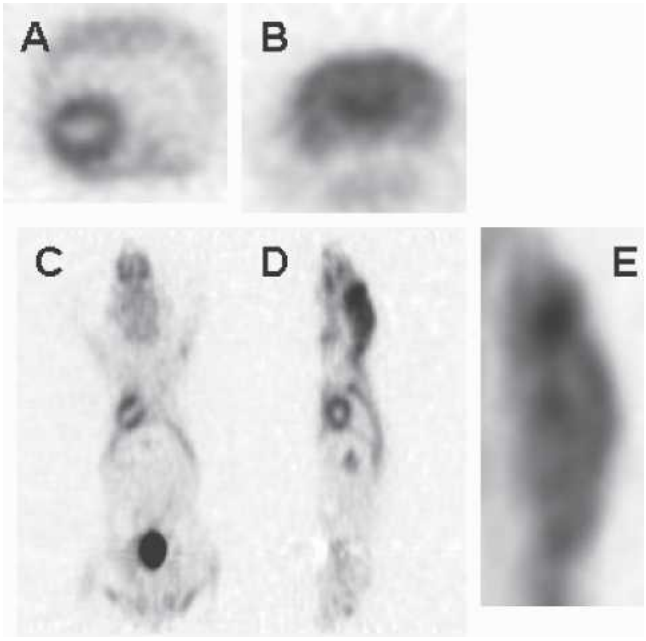

Figure 8 FDG accumulation in a 20-gram mouse. Approximately 0.5 mCi of FDG was administered via a tail-vein injection while the animal was awake. After a 45-minute uptake period the animal was anesthetized with isoflurane and a 15-minute PET image was acquired. Panels C and D are coronal and sagittal views of the whole body. Panel A shows a zoomed image through the heart. Panels B and E are zoomed orthogonal slices through the brain.

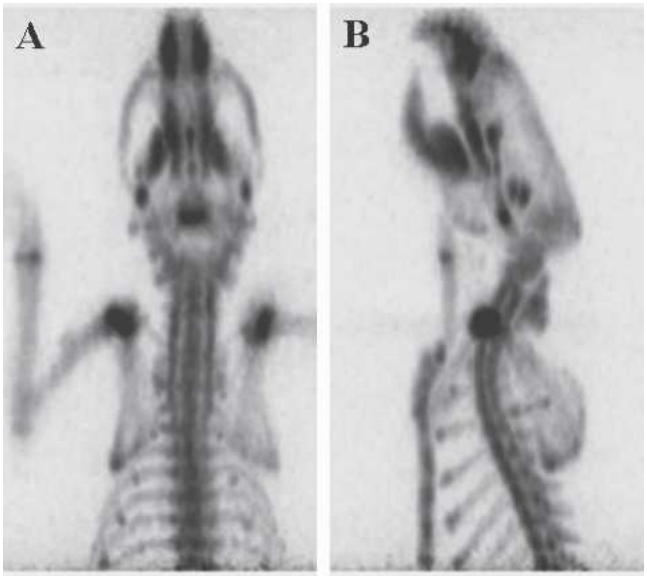

Figure 9 [F-18]fluoride uptake in the bone of a rat. The images are coronal (A) and sagittal (B) maximum intensity projection images of [F-18]fluoride retention in a 200-g rat. These images demonstrate the ability of state-of-the-art small animal PET systems to image small structures in the body. The [F-18]fluoride retention reflects bone perfusion and incorporation of F-18 into the bone matrix.

Figure 10 provides an example of cardiac imaging with small animal PET. The images in this figure demonstrate the ability to acquire cardiac-gated image data that facilitate an assessment of cardiac function along with cardiac biochemistry or biology. The image sets in Figure 10 used [C-11]carbon monoxide for blood pool imaging and FDG for assessment of glucose utilization by the myocardium.

Future Directions

Future efforts in small animal PET imaging technology will continue to push the limits of both spatial resolution and detection sensitivity. The anticipated benefits of high spatial resolution will not be achievable without significant advances in detection sensitivity. As shown in Figure 5 the RMSE increases dramatically as one pushes the spatial resolution limits of small animal PET. Overcoming the sensitivity limitation of very high spatial resolution in small animal PET will require novel detector designs (new scintillators and/or new geometrical designs) and advanced image reconstruction algorithms with a reduced sensitivity to the noise in the raw data collected by these systems. Advances in radiochemistry to optimize imaging agent–specific activity will also be a key factor in enabling the maximization of administered PET tracer doses for high-

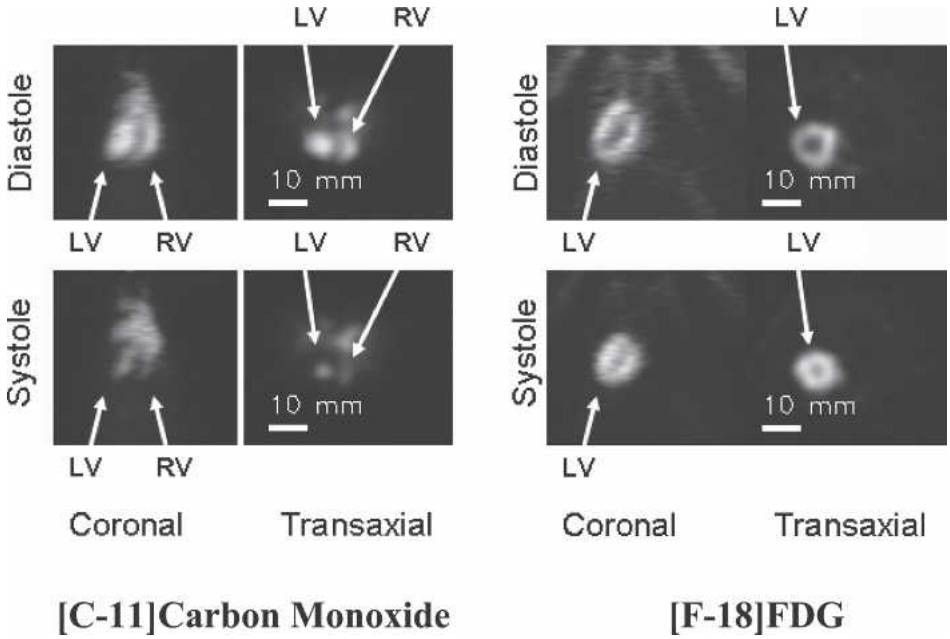

Figure 10 Gated cardiac images. The images on the left were created after the administration of [C-11]carbon monoxide, which binds to hemoglobin and produces an image of the body's red blood cell distribution. The images show changes in the volume of the chambers of the rat heart between systole and diastole. On the right are FDG uptake images during systole and diastole. These figures show the ability of small animal PET imaging to assess both the function of the heart as well as the underlying biology (metabolism in this example).

resolution applications. As with human PET imaging, there are ongoing efforts to integrate small animal PET with complementary imaging modalities, including optical and bioluminescence imaging, high-resolution CT imaging, and magnetic resonance imaging (MRI).

The ultimate utility of small animal and human PET imaging will depend on the availability of molecular imaging agents that target specific biological processes. Most PET tracers available today measure receptor expression or enzyme activity. While it is important to assess the alterations in receptors and enzyme function in disease, these are not typically the underlying processes that lead to disease. Therefore, one of the important future directions for PET imaging is targeting gene expression. Early efforts in this area include imaging of reporter genes (Blasberg 2002; Gambhir et al. 2000; Herschman et al. 2000), in which genes that express uniquely identified proteins or enzymes are incorporated into regulatory regions of genes of interest. A PET tracer specific to the reporter proteins is then used to examine the expression of the reporter over time. The long-range goal is to identify approaches that enable the assessment of gene expression without the need to transfect cells with reporter genes.

Summary

Small animal PET imaging is an evolving technology that makes it possible to probe biological processes in vivo using minimally invasive procedures. The size differences between humans and small animals present a formidable challenge in efforts to translate this technology from the human to preclinical imaging applications. Although the animals under study are much smaller than humans, the imaging systems are as complex as or more complex than clinical systems. There has been great progress in overcoming these limitations, and small animal PET imaging quality and quantitative imaging capabilities are now approaching those of human PET imaging.

A key driver for future advances in both human and small animal PET is the development of molecular imaging probes labeled with positron-emitting radionuclides that are specific to key biological processes associated with human diseases and disorders. It is likely that small animal PET, coupled with human PET imaging capabilities, will eventually provide an outstanding platform for translational science. Because the small animal and human PET technologies and methodologies provide essentially the same information, and because PET imaging studies of both humans and small animals are based on the same molecular imaging agents, knowledge gained in one area can rapidly be employed in the other.

The strong translational science potential of small animal and human PET holds great promise to dramatically advance our understanding of human disease. The assessment of molecular and functional processes using imaging agents as either direct or surrogate biomarkers will ultimately enable the characterization of disease expression in individual patients, facilitating tailored treatment plans whose effectiveness can be monitored in each subject.

References

Blasberg R. 2002. PET imaging of gene expression. Eur J Cancer 38:2137-2146.

Bloomfield PM, Myers R, Hume SP, Spinks TJ, Lammertsma AA, Jones T. 1997. Three-dimensional performance of a small-diameter positron emission tomograph. Phys Med Biol 42:389-400.

Brix G, Lechel U, Glatting G, Ziegler SI, Münzing W, Müller SP, Beyer T. 2005. Radiation exposure of patients undergoing whole-body dual-modality 18F-FDG PET/CT examinations. J Nucl Med 46:608.

Budinger TF, Derenzo SE, Greenberg WL, Gullberg GT, Huesman RH. 1978. Quantitative potentials of dynamic emission computer tomography. J Nucl Med 19:309.

Cherry SR. 2001a. Fundamentals of positron emission tomography and applications in preclinical drug development. J Clin Pharmacol 41:482-491.

Cherry SR. 2001b. Use of positron emission tomography in animal research. ILAR J 42:219-232.

Cherry SR. 2006. The 2006 Henry N. Wagner Lecture: Of mice and men (and positrons)—advances in PET imaging technology. J Nucl Med 47:1735-1745.

Cherry SR, Shao Y, Silverman RW, Meadors K, Siegel S, Chatziioannou A, Young JW, Jones W, Moyers JC, Newport D, Boutefnouchet A, Farquhar TH, Andreaco M, Paulus MJ. 1997. MicroPET: A high resolution PET scanner for imaging small animals. IEEE Trans Nucl Sci 44:1161-1166.

Cherry SR, Sorenson JA, Phelps ME. 2003. Physics in Nuclear Medicine. Philadelphia: WB Saunders.

Cutler PD, Cherry SR, Hoffman EJ, Digby WM, Phelps ME. 1992. Design features and performance of a PET system for animal research. J Nucl Med 33:595-604.

Defrise M, Gullberg GT. 2006. Image reconstruction. Phys Med Biol 51:R136-R154.

Del Guerra A, Di Domenico G, Scandola M, Zavattini G. 1998. YAP-PET: First results of a small animal positron emission tomography based on YAP:Ce finger crystals. IEEE Trans Nucl Sci 45:3105-3108.

Derenzo SE, Moses WW, Huesman RH, Budinger TF. 1993. Critical instrumentation issues for <2 mm resolution, high sensitivity brain PET. In: Uemura K, Lassen NA, Jones T, Kanno I, eds. Quantification of Brain Function: Tracer Kinetics and Image Analysis in Brain PET. Amsterdam: Elsevier. p 25-40.

Elsinga PH, van Waarde A, Visser TJ, Vaalberg W. 1998. Visualization of β-adrenoceptors using PET. Clin Positron Imaging 1:81-94.

Gambhir SS, Herschman HR, Cherry SR, Barrio JR, Satyamurthy N, Toyokuni T, Phelps ME, Larson SM, Balatoni J, Finn R, Sadelain M, Tjuvajev J, Blasberg R. 2000. Imaging transgene expression with radionuclide imaging technologies. Neoplasia 2:118-138.

Harpen MD. 2004. Positronium: Review of symmetry, conserved quantities and decay for the radiological physicist. Med Phys 31:57-61.

Herschman HR, MacLaren DC, Iyer M, Namavari M, Iyer M, Namavari M, Bobinski K, Green LA, Wu L, Berk AJ, Toyokuni T, Barrio JR, Cherry SR, Phelps ME, Sandgren EP, Gambhir SS. 2000. Seeing is believing: Non-invasive, quantitative and repetitive imaging of reporter gene expression in living animals, using positron emission tomography. J Neurosci Res 59:699-705.

Hoffman EJ, Phelps ME. 1976. An analysis of some of the physical aspects of positron transaxial tomography. Comput Biol Med 6:345-360.

Hoffman EJ, Huang SC, Phelps ME. 1979. Quantitation in positron emission computer tomography: 1. Effect of object size. J Comput Assist Tomogr 3:299-308.

Hume SP, Myers R. 2002. Dedicated small animal scanners: A new tool for drug development? Curr Pharm Des 8:1497-1511.

Jagoda EM, Vaquero JJ, Seidel J, Green MV, Eckelman WC. 2004. Experiment assessment of mass effects in the rat: Implications for small animal PET imaging. Nucl Med Biol 31:771-779.

Jeavons AP, Chandler RA, Dettmar CAR. 1999. A 3D HIDAC-PET camera with sub-millimeter resolution for imaging small animals. IEEE Trans Nucl Sci 46:468-473.

Knoll GF. 1979. Radiation Detection and Measurement. New York: John Wiley and Sons.

Kung MP, Kung HF. 2005. Mass effect of injected dose in small rodent imaging by SPECT and PET. Nucl Med Biol 32:673-678.

Lecomte R, Cadorette J, Rodrique S, Lapointe D, Rouleau D, Bentourkia M, Yao R, Msaki P. 1996. Initial results from the Sherbrooke avalanche photodiode positron tomography. IEEE Trans Nucl Sci 43:1952-1957.

Lewitt RM, Matej S. 2003. Overview of methods for image reconstruction from projections in emission computed tomography. Proceedings of the IEEE 91:1588-1611.

Marriott CJ, Cardorette JE, Lecomte R, Scasnar V, Rousseau J, van Lier JE. 1994. High-resolution PET imaging and quantitation of pharmaceutical biodistributions in a small animal using avalanche photodiode detectors. J Nucl Med 35:1390-1396.

McLarty K, Reilly RM. 2007. Molecular imaging as a tool for personalized and targeted anticancer therapy. Nature 81:420-424.

Miller MA, Rouze NC, Hutchins GD. 2003. Small animal PET imaging. In: Proceedings of the 8th ICATPP Conference on Astroparticle, Particle, Space Physics, Detectors and Medical Physics Applications, October 2003, Como, Italy (available at http://villaolmo.mib.infn.it/Conference2003.html).

Muehllehner G, Karp JS. 2006. Positron emission tomography. Phys Med Biol 51:R117-R137.

Paans AM, Vaalburg W. 2000. Positron emission tomography in drug development and drug evaluation. Curr Pharm Des 6:1583-1591.

Phelps ME. 2000a. Inaugural article: Positron emission tomography provides molecular imaging of biological processes. Proc Natl Acad Sci U S A 97:9226-9233.

Phelps ME. 2000b. PET: The merging of biology and imaging into molecular imaging. J Nucl Med 41:661-681.

Phelps ME. 2006. PET: Physics, Instrumentation and Scanners. New York: Springer Science + Business Media.

Phelps ME, Hoffman EJ, Mullani NA, Ter-Pogossian MM. 1975. Application of annihilation coincidence detection to transaxial reconstruction tomography. J Nucl Med 16:210-224.

Qi J, Leahy RM. 2006. Iterative reconstruction techniques in emission computed tomography. Phys Med Biol 51:R541-R578.

Rouze NC, Schmand M, Siegal S, Hutchins GD. 2003. Design of a small animal PET imaging system with 1 microliter volume resolution. IEEE Trans on Nucl Med 51:757-763.

Rouze, NC, Hutchins GD. 2003. Design and characterization of IndyPET-II: A high-resolution, high-sensitivity dedicated research scanner. IEEE Trans Nucl Sci 50:1491-1497.

Seidel J, Vaquero JJ, Green MV. 2003. Resolution uniformity and sensitivity of the NIH ATLAS small animal PET scanner: Comparison to simulated LSO scanners without depth-of-interaction capability. IEEE Trans Nucl Sci 50:1347-1350.

Sossi V, Ruth TJ. 2005. MicroPET imaging: In vivo biochemistry in small animals. J Neural Transm 112:319-330.

Surti S, Karp JS, Perkins AE, Cardi CA, Daube-Witherspoon ME, Kuhn A, Muehllehner G. 2005. Imaging performance of a-PET: A small animal PET camera. IEEE Trans Med Imaging 24:844-852.

Tai YC, Laforest R. 2005. Instrumentation aspects of animal PET. Ann Rev Biomed Eng 7:255-285.

Tai YC, Chatziioannou A, Siegel S, Young J, Newport D, Goble RN, Nutt RE, Cherry SR. 2001. Performance evaluation of the microPET P4: A PET system dedicated to animal imaging. Phys Med Biol 46:1845-1862.

Tai Y, Chatziioannou A, Yang Y, Silverman R, Meadors K, Siegel S, Newport DF, Stickel JR, Cherry SR. 2003. MicroPET II: Design, development and initial performance of an improved microPET scanner for small-animal imaging. Phys Med Biol 48:1519-1537.

Tai YC, Ruangma A, Rowland D, Siegel S, Newport DF, Chow PL, Laforest R. 2005. Performance evaluation of the microPET-Focus: A third

generation microPET scanner dedicated to animal imaging. J Nucl Med 46:455-463.

Vaalburg W, Hendrikse NH, de Vries EF. 1999. Drug development, radiolabelled drugs and PET. Ann Med 31:432-437.

van Waarde A, Elsinga PH, Anthonio RL, Visser TJ, Blanksma PK, Visser GM, Paans AMJ, Vaalburg W. 1995. Study of cardiac receptor ligands by positron emission tomography. In: van der Wall EE, Blanksma PK, Niemeyer MG, Paans AMJ, eds. Cardiac Positron Emission Tomography. Dordrecht: Kluwer Academic. p 171-182.

Wahl RL, Buchanan JW, eds. 2002. Principles and Practice of Positron Emission Tomography. Philadelphia: Lippincott Williams and Wilkins.

Watanabe M, Uchida H, Okada H, Shimizu K, Satoh N, Yoshikawa E, Ohmura T, Yamashita T, Tanaka E. 1992. A high resolution PET for animal studies. IEEE Trans Med Imaging 11:577-580.

Watanabe M, Okada H, Shimizu K, Omura T, Yoshikawa E, Kosugi T, Mori S, Yamashita T. 1997. A high resolution animal PET scanner using compact PS-PMT detectors. IEEE Trans Nucl Sci 44:1277-1282.

Weber S, Bauer A. 2004. Small animal PET: Aspects of performance assessment. Eur J Nucl Med Mol Imaging 31:1545-1555.

Weber S, Terstegge A, Herzog H, Reinartz R, Reinhart P, Rongen F, Muller-Garmer HW, Halling H. 1997. The design of an animal PET: Flexible geometry for achieving optimal spatial resolution or high sensitivity. IEEE Trans Med Imaging 16:684-689.

Wolbarst AB, Hendee WR. 2006. Evolving and experimental technologies in medical imaging. Radiology 238:16-39.

Ziegler SI, Pichler BJ, Boening G, Rafecas M, Pimpl W, Lorenz E, Schmitz N, Schwaiger M. 2001. A prototype high-resolution animal positron tomography with avalanche photodiode arrays and LSO crystals. Eur J Nucl Med 28:136-143.